Master Equation Analysis of Pressure-Dependent Atmospheric Reactions

John R. Barker*,† and David M. Golden*,‡

Department of Atmospheric, Oceanic and Space Sciences and Department of Chemistry, University of Michigan, Ann Arbor, Michigan 48109-2143, and Department of Mechanical Engineering, Stanford University, Stanford, California 94305

Received May 9, 2003

Contents

1. Introduction

Many reactions are both temperature and pressure dependent. The simplest examples are dissociation and isomerization reactions and, of course, their reverse. At the lower temperatures involved in atmospheric chemistry, it is these reverse processes of radical association that are often the most relevant. Other examples involve reactions that proceed via bound intermediates, where competition between collisional stabilization and reaction can manifest itself as a complicated dependence on pressure. The earth's atmosphere includes an enormous range of pressure and temperature conditions; thus, pressure-dependent reactions are found at virtually all altitudes from the surface to well over 100 km.

As experimental techniques and observational methods become more sophisticated, theoretical modeling methods must become more advanced. Master equations are a result of a marriage between chemical reactions and energy transfer. Each process has its own time scale. When the time scales are of the same order, both processes must be included in modeling experimental data, and master equations accomplish that purpose. In modeling the atmosphere, there is a great need for interpolating and extrapolating sparse laboratory data. Modeling using master equations is the most accurate way of accomplishing that purpose, but semiempirical methods are the most practical.

The purpose of this review is first to survey the general types of pressure-dependent reactions that are common in the earth's atmosphere and that can be modeled using master equation techniques; second, to give a brief outline of the theory of master equations; and third, to give some specific examples of master equation treatments of atmospheric reactions. Elsewhere, one can find surveys of atmospheric chemistry,[1−8] detailed discussions of master equation techniques,[9−14] and descriptions of semiempirical methods.[15−26] Here, each of these is surveyed briefly, in the context of atmospheric applications.

1.1. Classes of Pressure-Dependent Reactions

Reactions are pressure-dependent when the rate of collisional energy transfer is competitive with the rate of a chemical process that depends on internal energy. Even "inert" gases like argon (Ar) and nitrogen (N_2) participate in energy transfer. Since the rate of energy transfer depends on the total pressure (including "inert" gases), the overall reaction is pressure-dependent. In each of the following classes, energy transfer can compete with the reactive process. Each reaction class defined here is distinct, but the distinctions can become blurred in some cases.

1.1.1. Recombination/Decomposition Reactions

Examples:

$$NO_2^{\bullet} + NO_3^{\bullet} \leftrightarrow N_2O_5 \quad (1)$$

$$ClO^{\bullet} + ClO^{\bullet} \leftrightarrow Cl_2O_2 \quad (2)$$

Reactions like (1) are important in all regions of the atmosphere, while (2) is particularly important with respect to polar stratospheric chemistry. In recombination reactions (the forward direction), chemical energy is released and a highly vibrationally excited product is produced. If energy transfer is too

* Address correspondence to either author. E-mail: (J.R.B.) jrbarker@umich.edu; (D.M.G.) david.golden@stanford.edu.
† University of Michigan.
‡ Stanford University.

10.1021/cr020655d CCC: $44.00
Published on Web 10/24/2003

John R. Barker was born in Sewanee, Tennessee, and raised in Orlando, Florida. He earned a B.S. degree in chemistry from Hampden-Sydney College (1965) and a Ph.D. in physical chemistry at Carnegie-Mellon University (1969) under the supervision of Joe V. Michael. After postdoctoral research with B. S. Rabinovitch at the University of Washington and with Ralph E. Weston, Jr., at Brookhaven National Laboratory, he carried out basic research at SRI International, collaborating in part with David M. Golden and Sidney W. Benson. Since 1985, he has been Professor of Atmospheric Science and Professor of Chemistry at the University of Michigan. He has always been interested in the kinetics and dynamics of highly vibrationally excited molecules, whether in the atmosphere, in combustion, or in space. He has carried out experiments and calculations on molecular energy transfer, gas-phase and aqueous kinetics, and laser-induced chemistry and was involved in developing the hypothesis that polycyclic hydrocarbons are responsible for the unidentified infrared emission bands observed from interstellar dust clouds. He is currently focusing his efforts on aspects of multiwell, multichannel unimolecular reaction dynamics.

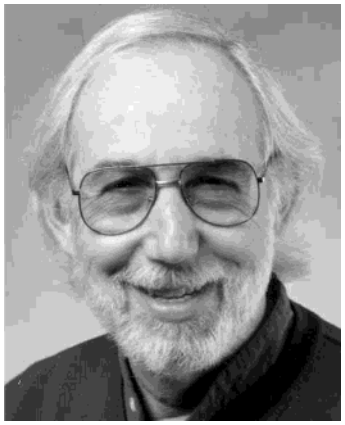

David M. Golden was born in Brooklyn, NY. He obtained an A.B. degree in chemistry from Cornell University (1956) and a Ph.D. in physical chemistry from the University of Minnesota (1960) under the supervision of Bryce L. Crawford, Jr. After a short postdoctoral fellowship at Princeton University with Donald F. Hornig, he entered the U.S. Army and worked at the Ballistic Research Laboratory in Aberdeen, MD, under the supervision of Frederick Kaufman. In 1963, he began a collaboration with Sidney W. Benson at Stanford Research Institute (now SRI International). He remained at SRI, serving as Chemistry Laboratory Director, Vice-President for Physical Science, and finally Sr. Vice-President for Science and where he still has some affiliation, until 1998, when he became a Consulting Professor at Stanford University in the Department of Mechanical Engineering. His research interests have always centered on chemical kinetics applied to practical problems, most notably with respect to the atmosphere and combustion. He has been a member since its inception of the NASA/JPL Panel that evaluates rate data for atmospheric models. He has also been a long-time member of the papers committee for the International Symposium on Combustion. He and his colleagues have performed experiments and calculations in many areas related to the above interests and have pioneered experimental techniques for examining gas–surface interactions of atmospheric interest that are in wide use today. He was Associate Editor of *The International Journal of Chemical Kinetics* from its founding in 1969 to 1976 and then Editor from 1983 to 1997.

slow, the excited product re-dissociates and there is no net reaction. If energy transfer is very fast, then the excited product is efficiently stabilized. The "falloff curve", representing the rate coefficient as a function of pressure at a given temperature, is a quantitative representation of the efficiency of stabilization as a function of the total pressure. Decomposition reactions are the reverse of recombination reactions: a stable molecule is activated by collisions and the highly vibrationally excited product decomposes. The efficiency of the collisional activation is described by the "falloff curve" describing the rate constant as a function of pressure at a given temperature. Falloff curves for recombination and decomposition reactions for the same chemical system are connected by microscopic reversibility and thus are described by the same physics and can be represented using the same functional forms.

1.1.2. Chemical Activation Reactions

In this general class, a bimolecular reaction leads to a single, highly vibrationally excited intermediate that is capable of further decomposition, isomerization, or collisional stabilization. The product branching ratio depends on pressure because collisional stabilization of the excited intermediate results in an increased yield of the stabilized intermediate at the expense of decomposition or isomerization products.

An example is the reaction between $CH_3^{\bullet}$ (methyl radicals) and $CH_2Cl^{\bullet}$ (chloromethyl radicals) to produce a highly excited CH_3CH_2Cl (ethyl chloride) molecule that contains the energy of the newly formed C−C bond. This species is highly excited with respect to elimination of HCl and formation of C_2H_4 (ethylene), a process with an energy barrier significantly lower than the energy of the C−C bond.

$$CH_3^{\bullet} + CH_2Cl^{\bullet} \rightarrow CH_3CH_2Cl^{*} \rightarrow HCl + C_2H_4 \quad (3)$$

1.1.3. Complex Bimolecular Reactions

This is a particular type of chemical activation system in which two chemical species react together to produce a short-lived, highly vibrationally excited intermediate complex that can decompose to produce new products, or re-dissociate to regenerate the original reactants. In the latter case, there is no net reaction; in the former case, the reaction appears to be a simple bimolecular process. If the intermediate complex undergoes collisional relaxation, re-dissociation is reduced and production of the new products is enhanced or the intermediate is stabilized. Because collisional relaxation is involved, the overall process is pressure-dependent. At ordinary pressures, the intermediate complex often cannot be isolated. An important example of reactions of this type is the reaction between hydroxyl radical (OH) and carbon monoxide (CO). The excited HOCO formed can return

to HO + CO or go on to H + CO_2 with similar ease.

$$OH\bullet + CO \Leftrightarrow HOCO^* \rightarrow H + CO_2$$
$$\Updownarrow M$$
$$HOCO$$

1.1.4. Chemical Excitation Reactions

In this special type of chemical activation, a bimolecular reaction produces a vibrationally excited product that undergoes subsequent reactions at an enhanced rate (due to the vibrational excitation). Collisional deactivation of the excited product affects the subsequent reactions. An important example of this class is found in part of the mechanism describing the atmospheric photo-oxidation of hydrofluorocarbon HFC-134a (1,1,2-tetrafluoroethane):

$$CF_3CFHO_2^\bullet + NO^\bullet \rightarrow CF_3CFHO^{\bullet *} + NO_2^\bullet \quad (4a)$$

$$CF_3CFHO^{\bullet *} \rightarrow CF_3^\bullet + FC(O)H \quad (4b)$$

$$CF_3CFHO^{\bullet *} + M \rightarrow CF_3CFHO^\bullet + M \quad (4c)$$

The vibrationally excited alkoxy radical ($CF_3CFHO^{\bullet *}$) decomposes at a faster rate than the thermalized radical ($CF_3CFHO^\bullet$), affecting the product branching ratio. Both radicals react with O_2 according to reaction (4d):

$$CF_3CFHO^\bullet + O_2 \rightarrow CF_3C(O)F + HO_2^\bullet \quad (4d)$$

In analyzing the experiments, it has been assumed that the rate of reaction (4d) does not depend on vibrational excitation. This assumption should be examined further in the future.

1.1.5. Multiwell, Multichannel Reactions

This reaction class includes reactions in which vibrationally excited species are produced by chemical activation, thermal activation, photoactivation, or some other process, and then undergo competitive reactions via several pathways with rates that depend on the excitation energy. Collisional deactivation slows the energy-dependent reaction rates and hence causes changes in branching ratios, etc.

Free radical isomerization/decomposition reactions fall into this category. In the atmosphere, alkoxyl radicals can undergo decomposition and isomerization reactions, which depend on vibrational energy, as well as bimolecular reaction with O_2. As mentioned above, it is not known whether the bimolecular reaction with O_2 depends on vibrational energy.

Another example involves nitrate formation in the reaction of alkyl peroxyl (or hydroperoxyl) radicals with NO. In this example, the two isomers formed, $RONO_2$ and ROONO, comprise the two wells. In addition to possible isomerization, there are two decomposition channels leading to either RO + NO_2 or RO_2 + NO. Since collisional deactivation competes with these processes, a full master equation calculation is needed in order to simulate this system.

2. Theory

2.1. Master Equation Calculations

Master equations describe quantitatively the simultaneous interplay of energy-dependent collisional energy transfer and energy-dependent chemical reactions. Such calculations are necessary for the most accurate descriptions of pressure-dependent reactions. Master equations of varying complexity are needed for the various classes of energy-dependent reactions listed above. The most complex pressure-dependent systems involve multiple potential energy wells and multiple reaction pathways. Although several methods have been developed for solving the resulting master equations, each method has strengths and weaknesses. Considerable work is needed to increase the speed and accuracy of the existing methods and to identify which methods are most suitable for certain classes of problems.

2.2. Master Equation Methods

Since the reaction rates are energy dependent and collisional energy transfer is not perfectly efficient, these atmospheric systems are best treated using master equation techniques. To implement the master equation model, parameters must be assigned for dissociation reactions, for isomerization reactions, and for energy transfer. The numerous parameters are assigned by using conventional unimolecular reaction rate theory, electronic structure calculations, and ancillary chemical kinetics data from the literature.

2.2.1. Rate Constant Expressions

In studies performed by the authors of this article of the reactions discussed herein, the MultiWell software package[13,27,28] was used for all of the calculations. Other software packages are available, however, including UNIMOL,[29] URESAM,[30] VariFlex,[31] ChemRate,[32] and UNIRATE.[33] In principle, each of the rate constants for dissociation and isomerization depends on vibrational energy and angular momentum, as does energy transfer. Typically a one-dimensional (vibrational energy) master equation treatment is employed with centrifugal corrections for angular momentum conservation. The centrifugal corrections are made using the pseudo-diatomic approximation[10] and by assuming the energy in the "K-rotor" (conserved rotational degree of freedom) is limited only by the total active energy and mixes freely with energy that resides in the other active degrees of freedom. These approximations are both accurate and commonplace.[11]

RRKM Theory. Unimolecular reaction rates are usually calculated using Rice−Ramsperger−Kassal−Marcus (RRKM) theory,[9−12] which requires calculation of the sums and densities of internal states for all of the potential wells and transition states. Electronic structure calculations can provide normal-mode vibrational frequencies and moments of inertia for the wells. In many cases, inspection of the normal-mode motions enables one to distinguish vibrational modes from the torsional modes, which can be treated as hindered internal rotations. The sums and densi-

ties of states can be calculated (program DenSum[28]) by "exact counts" using the Beyer−Swinehart algorithm[34] as adapted by Stein and Rabinovitch.[35]

According to RRKM theory,[9−12] the energy-dependent specific unimolecular rate constant $k(E)$ is given by

$$k(E) = \left[\frac{m^{\ddagger}}{m}\frac{\sigma_{\mathrm{ext}}}{\sigma_{\mathrm{ext}}^{\ddagger}}\right]\frac{g_{\mathrm{e}}^{\ddagger}}{g_{\mathrm{e}}}\frac{1}{h}\frac{G^{\ddagger}(E-E_0)}{\rho(E)} \qquad (5)$$

where $m^{\ddagger}$ and m are the numbers of optical isomers, $\sigma_{\mathrm{ext}}^{\ddagger}$ and σ_{ext} are the external rotation symmetry numbers, and $g_{\mathrm{e}}^{\ddagger}$ and g_{e} are the electronic state degeneracies of the transition state and reactant, respectively; h is Planck's constant, $G^{\ddagger}(E - E_0)$ is the sum of states of the transition state, E_0 is the reaction threshold energy, and $\rho(E)$ is the density of states of the reactant molecule. The internal energy E is measured relative to the zero-point energy of the reactant molecule, and the reaction threshold energy (critical energy) is the difference between the zero-point energies of reactant and transition state. Equation (5) was written by assuming that the rotational *external* symmetry numbers, electronic degeneracies, and numbers of optical isomers were *not* used in calculating the sums and densities of states. It is, however, assumed that *internal* rotor symmetry numbers are used explicitly in the sum and density calculations and hence do not appear in equation (5). Note that the quantity set off in square brackets is the reaction path degeneracy.

Centrifugal corrections to the unimolecular rate constants are made according to the pseudo-diatomic model, where the reaction threshold energy at a given temperature is corrected approximately for angular momentum effects by using a threshold energy, E_0^{T}, given by the following expression:[10,12]

$$E_0^{\mathrm{T}} = E_0 - k_{\mathrm{B}}T\left\{1 - \frac{I_{2\mathrm{D}}}{I_{2\mathrm{D}}^{\ddagger}}\right\} \qquad (6)$$

where $I_{2\mathrm{D}}$ and $I_{2\mathrm{D}}^{\ddagger}$ are the moments of inertia for the external two-dimensional (2-D) inactive (adiabatic) rotations of the reactant and of the transition state, respectively, and k_{B} is Boltzmann's constant. The resulting expression for $k(E)$ corresponds to that given by equation 4.31 in the book by Robinson and Holbrook[9] or equation 3.31 in the book by Holbrook, Pilling, and Robertson.[12]

For a thermal distribution, recombination reaction rate constants (k_{rec}) are related to the corresponding unimolecular rate constants (k_{uni}) according to the equilibrium constant (K). Thus, at the high-pressure limit we have the relationship

$$K = \frac{k_{\mathrm{rec}}^{\infty}}{k_{\mathrm{uni}}^{\infty}} \qquad (7)$$

Equilibrium constants can be calculated using the computer code Thermo,[28] which employs conventional statistical mechanics formulas for separable degrees of freedom that include harmonic and anharmonic oscillators, free and hindered internal rotors, and external rotational degrees of freedom.

In recombination reactions, the two reactants come together to form a highly excited adduct, which can re-dissociate, be collisionally deactivated, and react via other reaction channels. The chemical activation energy distribution[13] describes the nascent energy distribution of the complex formed in the recombination reaction:

$$y_0^{(\mathrm{ca},i)}(E)\,\mathrm{d}E = \frac{k_i(E)\rho(E)\,\mathrm{e}^{-(E/k_{\mathrm{B}}T)}\,\mathrm{d}E}{\int_{E_0}^{\infty}k_i(E')\rho(E')\,\mathrm{e}^{-E'/k_{\mathrm{B}}T}\,\mathrm{d}E'}, \quad \text{for } E \geq E_0 \qquad (8)$$

where $y_0^{(\mathrm{ca},i)}(E)$ is the energy distribution of molecules formed via reaction channel i, which has energy threshold E_0 and specific rate constant $k_i(E)$, $\rho(E)$ is the density of states in the new molecule, and the zero of energy for this equation is at the zero-point energy of the newly formed species.

Loose Transition States. For "loose" transition states, the properties of the transition state depend sensitively on angular momentum and the detailed shape of the interaction potential. In the absence of other information, it is possible to estimate the rate constant by using variational transition-state theory with a calculated potential energy surface.[11,36] When the rate constant is known, however, it is more convenient to use a "restricted" Gorin model with a "hindrance parameter" selected to reproduce the known rate constant for the corresponding reverse (recombination) reaction.[11,37,38]

According to the Gorin model,[39] the two molecular fragments rotate independently of one another while separated at the distance corresponding to the centrifugal maximum (r_{max}) of the effective potential of the bond being broken. For those systems with loose transition states considered herein, the rotations of both fragments and the overall transition state are treated approximately as symmetric tops. The overall transition state has a 2-D external adiabatic rotation with moment of inertia given by $I_{2\mathrm{D}}^{\ddagger} = \mu r_{\mathrm{max}}^2$, where μ is the reduced mass of the two fragments, and a 1-D external rotation (the "K-rotor") with moment of inertia I_{k}. The K-rotor is not adiabatic and is assumed, according to the usual approximation,[11] to mix energy freely with the active vibrations. The internal rotations of fragments A and B are characterized by 2-D rotations with moments of inertia I_{a} and I_{b}, respectively, and an internal rotation with reduced moment of inertia I_{r}. The moments of inertia I_{r} and I_{k} are obtained by combining the K-rotors of the individual fragments, as described by Gilbert and Smith.[11]

In the restricted Gorin model,[11,37,38] it is assumed that the two fragments interfere sterically with each other and thus cannot rotate freely. The effect is to reduce the available phase space and hence reduce the sum of states. Operationally, a "hindrance" parameter η is defined,[38] which can vary from zero (free rotation) to unity (completely hindered). The 2-D moments of inertia I_{a} and I_{b} are multiplied by the

factor $(1 - \eta)^{1/2}$ to obtain the effective 2-D moments of inertia used for calculating the sum of states.

In general, the potential function describing the breaking bond is not known, but the Lennard-Jones potential is often chosen for its simplicity and because it has the long-range dependence on r^{-6} expected for many long-range potentials. It does not describe a chemical bonding interaction very well at short range (near the potential minimum energy), however. For the Lennard-Jones potential, the moment of inertia for the two-dimensional adiabatic external rotation is given by $I^{\ddagger}_{2D} = \mu r_e^2 (6D_e/RT)^{1/3}$, where r_e is the equilibrium bond distance, μ is the reduced mass, and $D_e = D_0 - \Delta E_z$, where D_0 is the bond dissociation enthalpy at 0 K, ΔE_z is the zero-point energy difference between products and reactants, and R is the gas law constant. Use of Morse or Varshni potentials changes some fitting parameters, but not the qualitative result.

In another article in this issue (with extensive references to earlier work), Troe[18] espouses a somewhat different point of view. He argues that, given the potential energy surface, it is possible to compute the centrifugal partition function directly and then to calculate what he calls a rigidity factor that reflects the tightening of the transition state. The adequacy of the potential energy surface is always the open question.

2.2.2. Semiempirical Rate Constant Expressions

It has been the practice in both the atmospheric and combustion communities to represent unimolecular reactions (and their reverse) using analytical expressions put forth by Troe.[16]

The general format of these expressions is

$$k(M,T) = \left(\frac{k_0(T)[M]}{1 + (k_0(T)[M]/k_\infty(T))}\right)F \qquad (9)$$

The term in large brackets is the result of the simple Lindemann−Hinshelwood mechanism, and the factor F takes into account the fact that the energy dependence is more complicated than Lindemann−Hinshelwood, leading to a "broadening" of the curve. Troe further suggested that the F or "broadening factor" could be written as F_c^x, where the factor F_c is the broadening correction at the center of the falloff curve (i.e., when $k_0(T)[M] = k_\infty(T)$) and the quantity x is some function of the rate parameters and the pressure.

In the atmospheric community, there are two widely used compilations of rate data, one due to NASA[6] and the other to IUPAC.[5] These groups have used somewhat different versions of the Troe expression:

NASA Format

$$k(M,T) = \left(\frac{k_0(T)[M]}{1 + (k_0(T)[M]/k_\infty(T))}\right)0.6^{\{1+[\log(k_0(T)[M]/k_\infty(T))]^2\}^{-1}} \qquad (10)$$

IUPAC Format

$$k(M,T) = \left(\frac{k_0(T)[M]}{1 + (k_0(T)[M]/k_\infty(T))}\right) F_c^{\{1+[\log(k_0(T)[M]/k_\infty(T))/(0.75-1.27\log(F_c))]^2\}^{-1}} \qquad (11)$$

A third semiempirical equation is the J-Equation described by Oref,[19] which has been singled out by Hessler and Ogren[20] because the parameters show less correlation than the other semiempirical formulas used for fitting data:

J-Equation

$$k(M) = \{-(k_\infty + k_0) + [(k_\infty + k_0)^2 + 4(J-1)k_\infty k_0]^{1/2}\}[2(J-1)]^{-1} \qquad (12)$$

Like the IUPAC representation, the J-Equation requires three temperature-dependent parameters.

There are two obvious differences between the formulations based on Troe's approach. First, the NASA formulation assumes that, under atmospheric conditions, typically $200 < T/\mathrm{K} < 300$ and $1 < P/\mathrm{Torr} < 760$, $F_c = 0.6$ is a constant, while the IUPAC formulation suggests different values for each reaction. (This introduces an additional parameter into the formulations as written, but the IUPAC group often suggests that k_∞ is not temperature dependent, thus reducing the number of parameters.) Second, the IUPAC formulation takes into account the asymmetry expected in the falloff curve, although the term $[0.75 - 1.27 \log F_c]$ is very close to unity if $F_c = 0.6$, the value used in the NASA formulation and often suggested in the IUPAC recommendations.

If accurate and exceptionally precise data exist for any given process, the above formulations could be compared and the better representation might be ascertained. Rarely are data precise enough for such a test. On the other hand, theoretical methods might be useful in making such a distinction. In fact, it has been suggested that theoretical methods due to Troe[18] may be employed to predict k_0 and k_∞ so well that the ends of the falloff curve become fixed. If this is so, RRKM/master equation methods as implemented in codes such as MultiWell [13] can be used to obtain the curvature, and the two formulations can be tested against theory and data.

3. Examples

In what follows, the OH + NO_2, RO + NO_2, ClO + ClO, and OH + CO systems are examined using MultiWell in light of recent data. These systems are of great interest, and many workers have addressed the same issues. Earlier studies usually did not employ master equations, but more recently this has become the norm. The authors have done extensive work on these systems and will emphasize their own studies while attempting to adequately reference the efforts of others.

3.1. $RO_x + NO_x$

The reactions of $RO_x^{\bullet}$ with NO_x ($x = 1, 2$) constitute a system that is rich in interesting and important chemical reactions. They take place on potential energy surfaces similar to Figure 1. The generic reactions can be written as follows, where the four

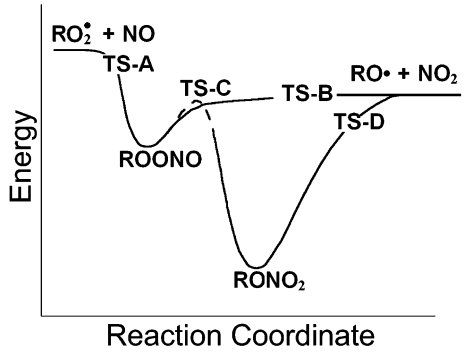

Figure 1. Schematic potential energy surface for the $RO_x + NO_x$ system.

transition states labeled in the figure correspond to the four reactions:

$$RO_2^\bullet + NO \leftrightarrow ROONO \quad (13)$$

$$RO^\bullet + NO_2 \leftrightarrow ROONO \quad (14)$$

$$ROONO \leftrightarrow RONO_2 \quad (15)$$

$$RO^\bullet + NO_2 \leftrightarrow RONO_2 \quad (16)$$

The combination of reactions (13) and (−14) gives a net reaction (17) that accounts for the reaction of peroxy radicals with nitric oxide to produce alkoxy radicals and NO_2. The combination of reactions (13) and (15) accounts for yields of alkyl nitrates under certain conditions, according to reaction (18). Reaction (16) is a key atmospheric free radical chain termination step. Transition states TS-A, TS-B, and TS-D are "loose", and the corresponding rate constants depend on angular momentum considerations.

$$RO_2^\bullet + NO \leftrightarrow RO^\bullet + NO_2 \quad (17)$$

$$RO_2^\bullet + NO \leftrightarrow RONO_2 \quad (18)$$

All of the reaction rates depend on vibrational energy, and the alkoxy radical product from reaction (17) is in many cases sufficiently vibrationally excited that it can decompose "promptly". Considering the complexities of this system, it is not surprising that master equation methods have been brought to bear on the interpretation of the relevant experimental data.

Three examples related to this reaction system are discussed in this section. First, the reaction of $OH^\bullet$ with NO_2 is a key reaction in the troposphere and stratosphere. Second, the prompt dissociation of alkoxy radicals produced in the ubiquitous atmospheric reaction of nitric oxide with peroxy radicals, which has important effects on product distributions, has received attention both experimentally and theoretically. Third, the production of alkyl nitrates in the reaction of peroxy radicals with nitric oxide continues to be a puzzle.

3.1.1. OH + NO_2

The reaction of OH with NO_2 is the principal sink for NO_x in the troposphere and thus has a direct effect on ozone production. In the stratosphere, nitric acid ($HONO_2$) is a "reservoir species", which "stores" highly reactive OH and NO_2 in a relatively inert form. In addition, the reaction is a popular test-bed for investigating fundamental aspects of recombination reactions. In experiments, OH radical can be detected with high sensitivity on very short time scales under an exceptionally wide range of experimental conditions. This has enabled experiments at temperatures from ∼220 to ∼450 K and pressures from ∼1 mbar to ∼1 kbar. Recent experiments have shown unambiguous evidence for the existence[40] and significant production of peroxynitrous acid (HOONO),[41] although its existence had been surmised earlier.[42−44] Recent spectroscopic results[45,46] have added support for the existence of HOONO. Thus, the reaction can be written with two channels:

$$OH + NO_2 \rightarrow HONO_2 \quad (19a)$$

$$\rightarrow HOONO \quad (19b)$$

A study by Golden, Lohr, and Barker[47] has applied MultiWell to interactions among the species OH, NO_2, $HONO_2$, and the two stable forms of HOONO, cis−cis HOONO and trans−perp HOONO. All molecular properties were from QCISD(T)/cc-pVDZ calculations. Hindered Gorin models were used for the bond-forming transition states, and calculations were performed to match data over wide temperature and pressure ranges with He and N_2 as bath gases. The extent of hindrance and the average amount of energy transferred were empirical parameters.

There is a large body of experimental data for this system. Much of it has been discussed in recent publications.[44,48−56] Some newer data have been published as well.[41,56] The data from Hippler and coworkers cleverly separates the two pathways forming $HONO_2$ and HOONO. To do this, the data were taken at 430 K and very high pressures (up to 130 bar). Figures 2−4 display some of the data in comparison with results from Golden, Lohr, and Barker.[47] The master equation fitted results can be described by several analytical schemes. One cannot easily distinguish among them. Table 1 gives the parameters corresponding to the NASA, IUPAC, and J-Equation formats given above.

The fractional yield of HOONO is presented in Figure 5 as a function of altitude, according to the three semiempirical fitting functions discussed above and the 1976 US Standard Atmosphere.[57,58] The results show that the yield of HOONO is a maximum near the tropopause, where the temperature is lowest and the pressure is still relatively high. At altitudes below about 50 km (the top of the stratosphere), the three fitting functions are in reasonable agreement, but at higher altitudes, the three fits diverge from

Table 1. Fitted Rate Constant Parameters[47] for Reactions (19a) and (19b)

	$k_0'(T) = k_0^{300}(T/300)^{-n}$		$k_\infty(T) = k_\infty^{300}(T/300)^{-m}$		$F_c(T) = F_c^{300}(T/300)^{-q}$		$J(T) = J^{300}(T/300)^{-r}$	
	k_0^{300}	n	k_∞^{300}	m	F_c^{300}	q	J^{300}	r
NASA								
$HONO_2$	1.8 (−30)	3.0	2.8 (−11)	0	0.6			
HOONO	9.1 (−32)	3.9	4.2 (−11)	0.5	0.6			
IUPAC								
$HONO_2$	1.9 (−30)	2.0	2.8 (−11)	0	0.60	0.5		
HOONO	1.1 (−31)	4.1	6.1 (−11)	0.1	0.34	0.3		
J-Equation								
$HONO_2$	2.3 (−30)	3.0	2.7 (−11)	0			6.8	0
HOONO	1.1 (−31)	3.1	6.9 (−11)	−0.8			24.8	−3.5

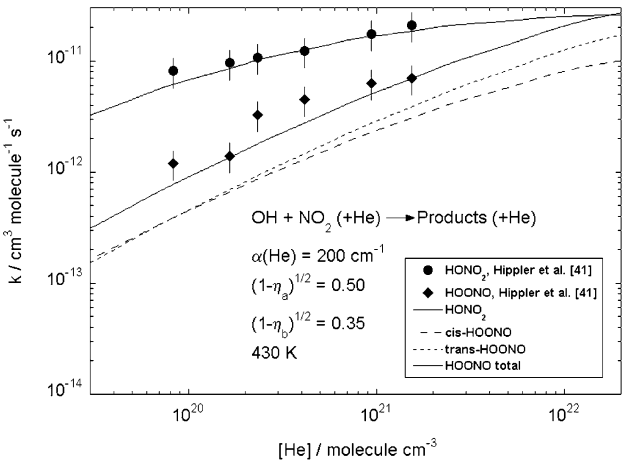

Figure 2. Data for the rate constant for the reaction between HO and NO_2 at 430 K in helium buffer gas, from various sources,[41,50,53,54,56] as indicated in the figure legend. The lines are the interpolated results of master equation calculations for $HONO_2$ formation and for formation of the indicated HOONO species.[47]

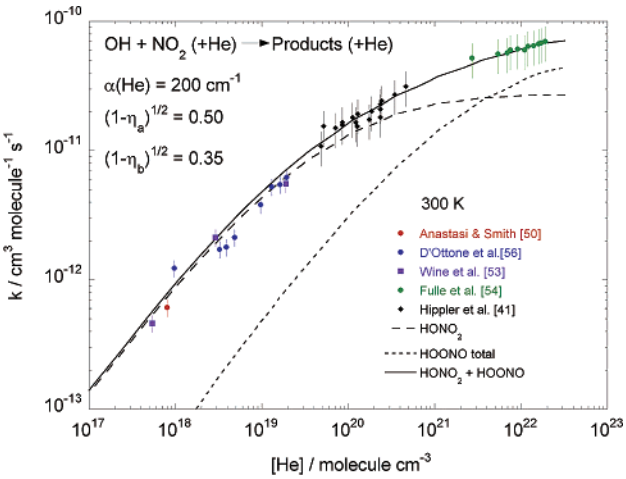

Figure 3. Data for the rate constant for the reaction between HO and NO_2 at 300 K in helium buffer gas, from various sources,[50−53,55,56] as indicated in the figure legend. The lines are the interpolated results of master equation calculations for $HONO_2$ formation and for formation of the indicated HOONO species.[47]

each other. At the low pressure limit, the fractional yield of HOONO is expected to become essentially constant.

3.1.2. Alkoxy Radical Reactions

Because of their contribution to destruction of the ozone layer,[59] chlorofluorocarbons (CFCs) are being

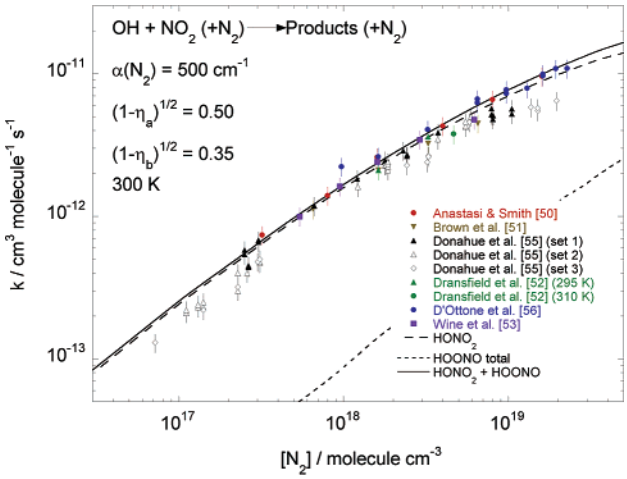

Figure 4. Data for the rate constant for the reaction between HO and NO_2 at 300 K in nitrogen buffer gas, from various sources,[50−53,55,56] as indicated in the figure legend. The lines are the interpolated results of master equation calculations for $HONO_2$ formation and for formation of the indicated HOONO species.[47]

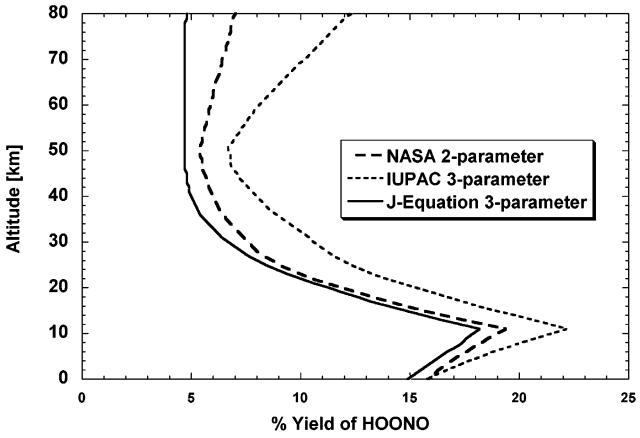

Figure 5. Predicted relative yield of HOONO as a percentage of the total rate of the OH + NO_2 reaction as a function of altitude,[47] based on the U.S. Standard Atmosphere, 1976.[57,58]

phased out of production and being replaced with environmentally acceptable alternatives. An important replacement compound is hydrofluorocarbon 134a (1,1,1,2-tetrafluoroethane), which is being used in air conditioning and refrigeration systems. HFC-134a itself has little effect on stratospheric ozone[60] and global warming,[61] but when degraded in the atmosphere it produces trifluoroacetic acid, which is phytotoxic[62] and may accumulate with time.[63] During

investigations of the atmospheric chemistry of HFC-134a, two puzzles emerged. First, the reaction rate constant for unimolecular reaction differs dramatically when the radicals are produced via disproportionation reaction (22), rather than via reaction (23):

$$CF_3CFHO^\bullet + M \rightarrow CF_3 + HC(O)F + M \quad (20)$$

$$CF_3CFHO^\bullet + O_2 \rightarrow CF_3COF + HO_2 \quad (21)$$

$$CF_3CFHO_2^\bullet + CF_3CFHO_2^\bullet \rightarrow 2CF_3CFHO^\bullet + O_2^\bullet \quad (22)$$

$$CF_3CFHO_2^\bullet + NO \rightarrow CF_3CFHO^\bullet + NO_2 \quad (23)$$

This puzzle can be explained if a significant fraction of the $CF_3CFHO^\bullet$ radicals produced in reaction (23) are vibrationally excited, but radicals produced in reaction (22) are not. Reaction (23) is significantly more exothermic than reaction (22), based on calculated heats of formation for fluorinated free radical species.[64−69] Since the barrier to C−C bond scission has been estimated to be lower than the exothermicity of reaction (23), the nascent alkoxy radical products may have enough energy to decompose prior to collisional stabilization and hence undergo "prompt" decomposition.[70−74] Experimental evidence is consistent with ∼60% of the nascent $CF_3CFHO^\bullet$ radicals undergoing decomposition promptly enough so that reaction (22) cannot compete.[60,75] Thus, reaction (23) must be replaced by reactions (23′), (24), and (25).

$$CF_3CFHO_2^\bullet + NO \rightarrow CF_3CFHO^{\bullet *} + NO_2 \quad (23')$$

$$CF_3CFHO^{\bullet *} \rightarrow CF_3^\bullet + HC(O)F \quad (24)$$

$$CF_3CFHO^{\bullet *} + M \rightarrow CF_3CFHO^\bullet + M \quad (25)$$

where the asterisk denotes internal excitation.

The implications of this result are much broader than just the reactions of $CF_3CFHO^\bullet$ radicals: the formation of alkoxy radicals via the generic reaction (26) is extremely important throughout the atmosphere. If subsequent reactions of excited alkoxy radicals ($RO^{\bullet *}$, where the asterisk denotes internal excitation) are enhanced, current atmospheric chemistry models will require major revision.

$$RO_2^\bullet + NO \rightarrow RO^{\bullet *} + NO_2 \quad (26)$$

Several groups have used master equation techniques to investigate the production of alkoxy radicals via reaction (26), and subsequent reactions of the excited radicals. Schneider et al.[65] carried out several levels of electronic structure calculations and combined them in an additive scheme in order to estimate the thermochemistry, vibrational frequencies, and structures of the chemical species related to $CF_3CFHO^\bullet$ radical decomposition. They modeled the reaction using RRKM theory and an exponential model for energy transfer. The calculated barrier to C−C bond fission via reaction (24) was 10.7 kcal mol^{-1}, and the exothermicity of reaction (23) was estimated to be 17 kcal mol^{-1}.[64] Since the energy distribution of the $CF_3CFHO^{\bullet *}$ radical subsequent to reaction (23′) was unknown, Schneider et al. approximated it as a thermal distribution at ambient temperature, displaced upward by a nominal excitation energy. Although relatively crude, this approximation captured the essential physics of the reaction system.

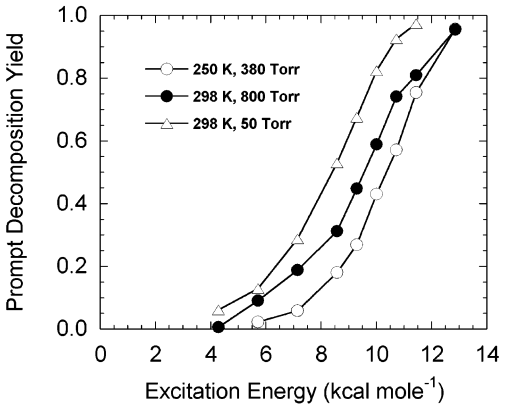

Figure 6. Prompt decomposition of chemically activated CF_3 $CFHO^{\bullet *}$ radicals. Adapted from ref 65.

Considering that there are 27 vibrational degrees of freedom in the $CF_3CFHO-O-NO$ transition state and only 18 vibrations in $CF_3CFHO^\bullet$, a statistical redistribution of the exothermicity would lead to an excitation energy of ∼11 kcal mol^{-1}. Schneider et al.[65] carried out calculations to determine the "prompt" decomposition yield as a function of the excitation energy and found that an excitation energy in the range from 9 to 11 kcal mol^{-1} is consistent with the experimental yield of ∼60%,[75] as shown in Figure 6.

Other workers have been using master equations to investigate alkoxy radical reactions. For example, Dibble[76] has carried out electronic structure calculations on the hydroxy-alkyl radicals formed from addition of OH radical to the double bonds in isoprene. The hydroxy-alkoxy radicals that are produced as a result of reactions with O_2 and nitric oxide can isomerize and decompose via several reaction channels. Dibble used MultiWell[13,77] to investigate the effects of quantum mechanical tunneling on these complicated mechanisms.

Somnitz and Zellner[69] carried out a systematic theoretical analysis of $CF_3CY_2O^\bullet$ (Y = F, H) radicals. They used an approach somewhat similar to that employed by Schneider et al.,[65] but which differed in details. In particular, they employed a different level of electronic structure calculations, estimated the assumed displaced−thermal distribution differently, and compared their model results to a wider range of experimental data. They estimated the critical energy of the bond dissociation reaction to be 12.1 kcal mol^{-1} and the excitation energy to be in the range from 13 to 14 kcal mol^{-1}, in reasonable agreement with the experimental data. In addition, they found that $CF_3CF_2O^\bullet$ radicals dissociate so rapidly that other reactions cannot compete, regardless of any excitation energy from reaction (17). In contrast, $CF_3CH_2O^\bullet$ radicals have such a high barrier to dissociation that excitation energy from reaction (17) still has little effect. Thus, one must conclude that

only certain halogenated species will show effects due to chemical activation via reaction (17).

Other groups have improved the model for prompt decomposition of chemically activated alkoxy radicals by using Wittig's separate statistical ensembles (SSE) model[78,79] to estimate the energy distribution function in the excited radicals produced by reaction (17). For example, Vereecken, Peeters, and co-workers[80−83] have used their stochastic master equation computer code[30] and the SSE model to estimate the extent of prompt decomposition of the alkoxy radicals. They have concluded that prompt decomposition of many of the excited radicals derived from biogenic hydrocarbons is very important, and even dominant, with respect to reaction with O_2, at low temperatures. Because the prompt reaction is the result of vibrational excitation that is degraded by competitive collisional deactivation, a master equation approach provides the best estimates of the effect. Note that this vibrational energy distribution function has never been measured experimentally: an important challenge!

Somnitz and Zellner[84−86] have carried out an extensive theoretical study of alkoxy radical unimolecular reactions. First, they carried out electronic structure calculations using several levels of theory.[84] The electronic theory results were used to calculate specific rate constants and falloff curves using RRKM theory,[86] and the results of those calculations were used to develop a structure−activity relationship for predicting the energy barriers for linear alkoxy radicals of arbitrary length.[85]

One of the most interesting aspects of the work of Somnitz and Zellner[86] is the investigation of the competitive coupling among reaction pathways in multichannel unimolecular reaction systems. A good example the 2-pentoxy radical:

$$CH_3{-}CH(O^{\bullet}){-}CH_2CH_2CH_3 \rightarrow CH_3^{\bullet} + CH(O)CH_2CH_2CH_3 \quad (27a)$$

$$\rightarrow CH_3CH(O) + {}^{\bullet}CH_2CH_2CH_3 \quad (27b)$$

$$\rightarrow CH_3CH(OH)CH_2CH_2CH_2^{\bullet} \quad (27c)$$

Reactions (27a) and (27b) produce a carbonyl and a free radical; reaction (27c) is a "tail-biting" isomerization via a six-center transition state. The coupling takes place because of competition for the high-energy population, which is rapidly depleted by low-energy (fast) reactions, hence making it unavailable for the reactions with higher energy barriers. For 2-pentoxy radical, reaction (27c) has the lowest energy barrier. In all cases, the lowest energy reaction is not affected significantly by the higher energy pathways, but the reactions with higher energy barriers are severely affected by the lower energy paths. Somnitz and Zellner found that it is possible to fit their master equation results for the lowest energy channel to the semiempirical functions described by Troe.[15,16] Fits of the Troe functions to the higher energy channels cannot be very accurate, however, because the competitive coupling produces falloff curves that are higher than first order with respect to pressure at the low-pressure limit, as pointed out for reactions alkyl radicals.[27] This same high-order behavior is apparent by inspection of Figures 4−7 in the article by Somnitz and Zellner.[86]

3.1.3. Alkyl Nitrate Formation

In 1976, Darnall et al.[87] reported that the reaction of alkyl peroxy radicals ($RO_2^{\bullet}$) with nitric oxide produces not only alkoxy radicals ($RO^{\bullet}$) and NO_2, but also a significant yield of alkyl nitrates:

$$RO_2^{\bullet} + NO \rightarrow RO^{\bullet} + NO_2 \quad (28a)$$

$$\xrightarrow{M} RONO_2 \quad (28b)$$

This result is important because alkyl nitrates are relatively inert in the troposphere,[88] and therefore reaction (28b) is a sink for both $RO_2^{\bullet}$ radicals and NO_2, the direct precursor of ozone; when NO_2 is removed, less ozone is produced. The discovery of reaction (28b) was surprising, because to form alkyl nitrates, the O−O bond in the $RO_2^{\bullet}$ radical must be broken and two new O−N bonds must be formed. This internal molecular rearrangement requires a three-center cyclic transition state, which is expected to have a very high energy barrier to reaction.[37] There is little doubt, however, that nitrates are formed via reaction (28b), since significant reaction yields have been measured in both static and flowing systems by numerous analytical methods.[88−91]

The potential energy surface (PES) shown in Figure 1 is essentially the same as the kinetics scheme postulated by Atkinson et al.[92] to explain the experimental data. The major features of the PES have been confirmed by calculations for R = H,[47,93−98] alkyls,[98,99] and hydroxy-substituted alkyls derived from isoprene.[100] The transition-state structure TS-C has not yet been positively located, although Dixon et al.[96] and Ellison et al.[99] have identified potential candidates.

Master equation calculations have been carried out by at least two groups with the aim of investigating the formation of alkyl nitrates. Zhang et al.[100] investigated nitrate and nitrite formation in the OH-initiated reactions of isoprene. They first carried out extensive quantum chemical calculations to characterize the reaction thermochemistry, structures, and vibrational frequencies. Because $OH^{\bullet}$ radical can attack at either end of the two double bonds in isoprene, four structural isomers of $RO_2^{\bullet}$ are formed, and each can assume any one of a number of rotational conformations. An interesting aspect is the internal hydrogen bonding that occurs in the β-ROONO isomers, leading to added stability. Zhang et al. treated the loose transition states by using variational RRKM theory, based on a Morse potential. The calculated high-pressure limit rate constants for the RO_2 + NO reaction ranged from $\sim 3 \times 10^{-12}$ to 13×10^{-12} cm^3 s^{-1}, in reasonable agreement with literature values[3,4] for similar reactions.

Because the structure of transition state TS-C is not known from calculations, Zhang et al.[100] considered two limiting cases. In the first case, Zhang et

al. assumed that the TS-C structure and vibrational frequencies are the same as for ROONO itself: a moderately tight transition state. In the second case, they assumed that TS-C has the same properties as transition state TS-B: a loose transition state. Using these two cases, they fitted a set of room temperature, atmospheric pressure hydroxy-alkyl nitrate yield data[101] with isomerization barriers that ranged from ~7 to 13 kcal mol^{-1}. For comparison, the calculated RO−ONO bond dissociation energies range from 7.5 to 9.4 kcal mol^{-1}, much lower than the calculated ROO−NO bond energy of ~20 kcal mol^{-1}.

Barker, Lohr, and co-workers[98,102] carried out electronic structure and master equation calculations on alkyl nitrate systems with R = CH_3, *i*-C_3H_7, and 2-C_5H_{11}. The original aim of the work was to construct a semiempirical master equation model for alkyl nitrate formation that could be used for predictions. They employed hindered Gorin models[11,37,39,44,103] for the loose transition states, based on the approach of Smith and Golden,[38] with hindrance parameters adjusted to make the rate constants match experimental data. It was assumed that the rate constant for reaction (14) is the same as the experimental rate constant for reaction (18), and that in the reaction between RO$^\bullet$ and NO_2, reaction with each atom of the NO_2 is equally likely. Various assumptions about transition state TS-C were investigated, including the use of a vibrational model and Forst's inverse Laplace transform model[10,104] with assumed activation energies and *A*-factors. Except for the energy of TS-C, the thermochemistry was held fixed at the "generic" alkyl values identified by Lohr et al.[98]

Generally speaking, Barker et al.[102] found that experimental alkyl nitrate yields at single fixed pressures could be modeled with relative ease by varying transition-state and energy-transfer parameters, but fitting an entire set of pressure-dependent yields[105,106] was much more difficult and could only be achieved by using parameters in the master equation model that were surprising and perhaps unphysical. An example of master equation fits to the temperature- and pressure-dependent yields of 2-pentylnitrate[105,106] is presented in Figure 7. The agreement with the experimental data is very good, including both the pressure and temperature dependence. However, the agreement could only be achieved by using energy transfer parameter $\alpha = 25$ cm^{-1}, as illustrated in Figure 8.

This magnitude of energy transfer parameter α is exceptionally small, only about one-tenth of the expected value. Physical measurements of toluene deactivation[14,107] gave 270 cm^{-1} (for N_2 collider gas) at the same internal energy, which can be compared with ~500 and ~1000 cm^{-1} obtained for $HONO_2$ (Golden et al.[47]) and CH_3ONO_2 (see above and Barker et al.[102]), respectively. Because the properties of the loose transition states are not independently constrained, the value of α may vary over a wide range, perhaps accounting for its exceptionally small magnitude. Nevertheless, this small value of α may signal that there are errors in the pressure-dependent data, or that there are important problems with the master equation model. Since the data were obtained only in a single laboratory and with a single experimental technique, it would be appropriate for new experiments to be carried out, prior to further attempts at master equation modeling of this system.

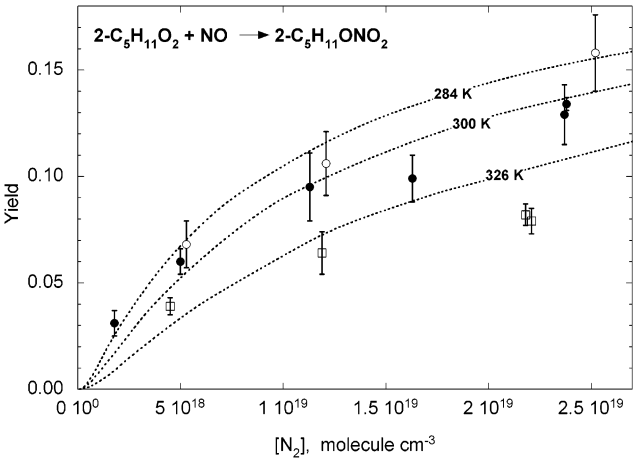

Figure 7. 2-Pentylnitrate yields as a function of temperature and nitrogen concentration. Data are from Atkinson et al.,[105,106] and lines are model calculations[102] using α = 25 cm^{-1}, critical energy E_0 = 52.5 kJ mol^{-1}, and $A_\infty = 6.3 \times 10^{16}$ s^{-1}.

3.2. ClO + ClO

When depletion of polar ozone in Austral Spring was first brought to the community's attention, there was uncertainty as to the mechanism. An aspect of this uncertainty reflected the concern that the atmosphere, emerging from the long polar night, did not have a sufficient concentration of O atoms to take part in the normal global ClO_x cycle for ozone depletion. It has been suggested that, under these conditions, the reaction of two ClO radicals to form the peroxy dimer, ClOOCl, which then photolyzes to Cl + ClOO, the ClOO subsequently yielding another Cl and O_2, would be a sufficient source of Cl atoms. This has prompted some detailed studies of this reaction. Golden[108] has attempted to reconcile all the extant data[109,110] and theoretical calculations using both MultiWell and psuedo-strong collision RRKM theory.

Potential energy surface calculations by Lin and co-workers[111] reveal the possibility of the formation of ClOClO. In the study by Golden, RRKM/master equation modeling of this surface has been performed. Rational input parameters confirm that the formation of ClOClO in 10−15% yields may be important, but they do not conform with the shape and temperature dependence of the data. The simplest best representation of the extant data remains the single-channel NASA/JPL format with parameters $k_0 = 1.6 \times 10^{-32}(T/300)^{-4.5}$ cm^6 molecule^{-2} s^{-1} and $k_\infty = 2.0 \times 10^{-12}(T/300)^{-2.4}$ cm^3 molecule^{-1} s^{-1}. However, the data can be represented as the sum of the two pathways as well. It has been suggested[48] that the mechanism might include participation of bound complexes of ClO with bath gas and that this could reconcile the data. Figure 9 shows the data, illustrating the essential agreement between the two studies shown. Also illustrated are the best fits using a single reaction channel.

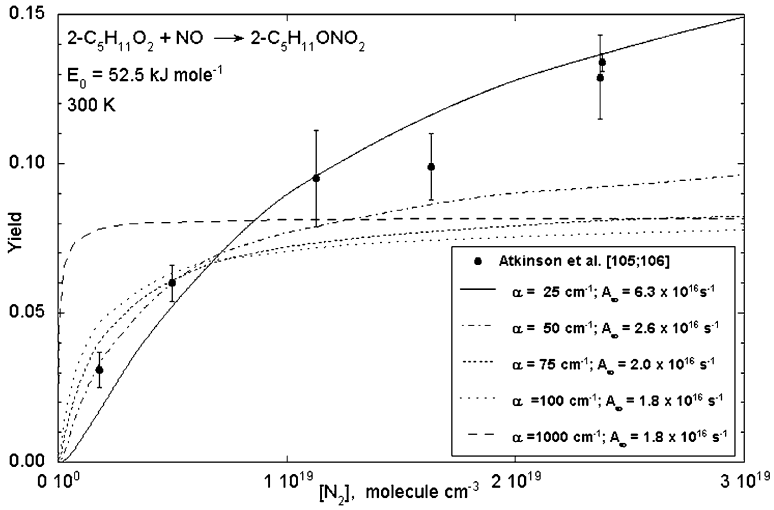

Figure 8. Yield of 2-$C_5H_{11}ONO_2$ at 300 K. Data (points) are from Atkinson et al.[105,106] Model calculations[102] with the critical energy $E_0 = 52.5$ kJ mol^{-1} and *A*-factors given in the figure legend.

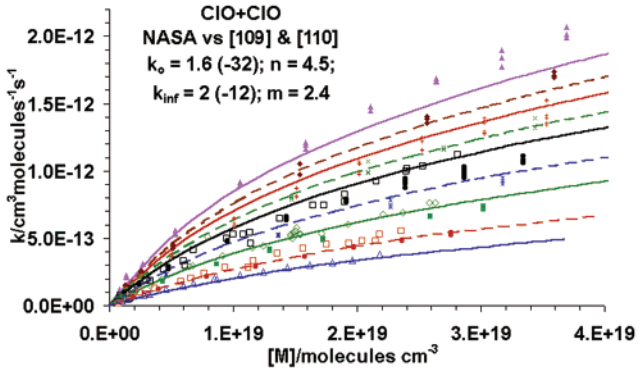

Figure 9. Data and NASA/JPL parameters for the reaction of ClO with ClO. Closed symbols, Bloss et al.;[109] open symbols, Trolier et al.[110] Color code: magenta, 183 K; brown, 188 K; red, 192 K; green (dashed), 197 K; black, 200 K; blue (dashed), 213 K; green, 224 K; red (dashed), 245 K; blue, 263 K.

3.3. OH + CO

The reaction of carbon monoxide with hydroxyl radicals is of vital importance for combustion and atmospheric processes. In the case of hydrocarbon combustion, this is the main mechanism for converting CO into CO_2 and is responsible for a major fraction of the energy release. In the lower atmosphere, this reaction is implicated in smog formation by regulating the concentration of hydroxyl radicals that play a crucial role in NO_x and HO_x chemical cycles.

Due to its importance and its unusual temperature and pressure behavior, this system has inspired a large body of work, both theoretical and experimental. The temperature dependence presents two regimes with markedly different activation energies with a transition around 500 K.

In 1964, Ung and Back postulated the existence of the hydroxyoxomethyl radical (HOCO) radical as an intermediate in the addition of OH and CO.[112] Dryer, Naegeli, and Glassman[113] showed that transition state theory can predict the strong non-Arrhenius behavior of this reaction if the activation barrier is close to zero. The role of the collisional stabilization of HOCO and the complicated temperature and pressure dependence of this reaction were studied by Smith and Zellner[114] and Smith,[115] who proposed the general reaction mechanism illustrated earlier.

The currently accepted reaction mechanism consists of an OH + CO association step, forming *trans*-HOCO, followed by facile cis−trans isomerization and finally a decomposition step to H + CO_2. At moderate pressures, stabilization of HOCO intermediates competes with the decomposition channel and the back reaction to OH + CO. It is interesting to note that, when OH and CO react in air, both reaction channels eventually lead to the same final products, namely, HO_2 + CO_2, because both H atoms and HOCO react with O_2 to produce HO_2.

The existence of HOCO and DOCO has been confirmed with matrix-isolation techniques,[116] photoionization mass spectroscopy,[117,118] and ultrafast laser spectroscopy[119] of the OH radical produced in the reverse reaction of H + CO_2. The vibrational and rotational spectra of these radicals have been characterized.[120−124]

The heat of formation of the HOCO intermediates, relative to the OH + CO entrance channel, is of some importance for kinetic calculations in the falloff regime. Until recently, the accepted well depth of the *trans*-HOCO intermediate was presumed to be 35.4 kcal/mol below the OH + CO level, based on a $\Delta_f H^0_{298K}$(*trans*-HOCO) = −52.5 kcal/mol from photoionization studies.[118] However, more recent measurements[117] have set an upper limit of $\Delta_f H^0_{298K}$(*trans*-HOCO) > −46.5 kcal/mol, implying a *trans*-HOCO well depth of 28.9 kcal/mol at most [note that the heat of formation of OH was recently revised[125]]. This is consistent with lower well depths of more recent ab initio calculations.[126−128]

The reaction of OH with CO has been the subject of several theoretical and experimental investigations. Thermal reaction rate constants for this reaction have been measured at temperatures as high as 2800 K[129,130] and as low as 80 K.[131−133] For a concise summary of earlier work, see refs 134−136.

Early attempts[115,132,137−139] to model the reaction of CO and OH radicals based on RRKM theory and a

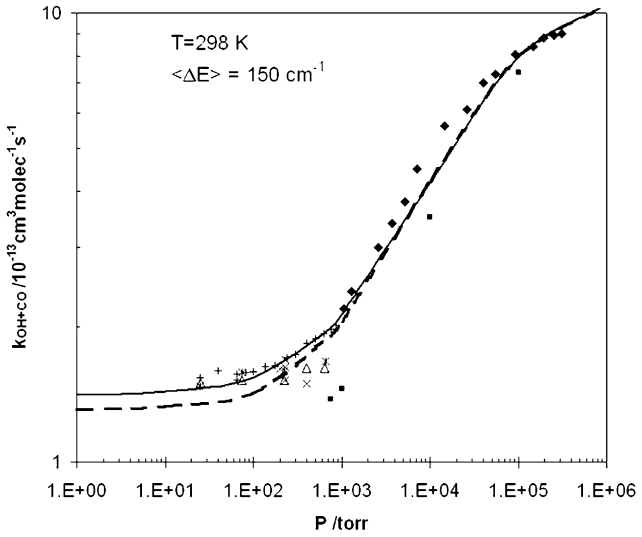

Figure 10. Falloff curve for OH• + CO in He bath gas at 298 K. Symbols represent experimental data;[131,142,147−149] see original publication[142] for symbol definitions. Lines represent RRKM calculations: He bath gas with ZCT (solid line) and without tunneling corrections (dashed).[142]

pseudo-strong collision approximation failed to predict the nearly temperature-independent rate constant below 500 K. Three more-recent studies have modeled this reaction, claiming to fit experimental rate coefficients to temperatures down to 80 K. Fulle et al.[131] and Troe[140] performed *E*- and *J*-resolved RRKM calculations with a pseudo-strong collision energy transfer model. They fit high- and low-pressure rate coefficients to optimize the PES of Kudla et al.[141] and reported that the two competing channels for HOCO dissociation (OH + CO and H + CO_2) are responsible for the observed biexponential decay of OH. Zhu et al.[128] performed a RRKM/master equation study based on their G2M surface, and attributed the unusually high low-temperature rate coefficients to a pronounced tunneling effect. They noted, however, that the magnitude of Wigner tunneling corrections is very sensitive to the imaginary frequency of TS2, which varies greatly depending on the method of calculation.

In 1998, Golden and co-workers[142] used statistical methods to fit the existing experimental data, optimizing the controlling barriers and the vibrational frequencies of *trans*-TS1 from ref 143. This fit yielded an optimized energy of *cis*-TS2 slightly below the entrance channel. A study by Senosiain et al.[144] attempts to generate a physically based model that reproduces the large body of experimental data and allows for reliable extrapolations to unknown conditions. In addition, parameters for use in atmospheric and combustion models are presented.

Rate calculations presented in the article by Senosiain et al.[144] were carried out using the potential energy surface of Yu and co-workers.[127] This surface is based on ab initio calculations done at the CCSD(T)/cc-pvTZ level and extrapolated to the infinite coupled-cluster limit and complete basis set.

Table 2. Optimized Parameters[142] for the Two Channel Rate RRKM/Master Equation Calculations in the Range 175 < *T*/K < 300 and 0 < P_{N_2}/Torr < 800

reaction	rate constant	k_{300}[a]	m[a]
CO+OH → HOCO	k_∞/cm^3 molecule^{-1} s^{-1}	1.13×10^{-12}	−1.32
	k_0/[*M*]/cm^6 molecule^{-2} s^{-1}	5.87×10^{-33}	+1.36
OH + CO → H + CO_2	k_∞/[*M*]/s^{-1}	2.12×10^{-9}	−6.08
	k_0/cm^3 molecule^{-1} s^{-1}	1.50×10^{-13}	−0.58

[a] Functional form: $k(T) = k_{300}((T/300))^{-m}$; $F_c = 0.6$.

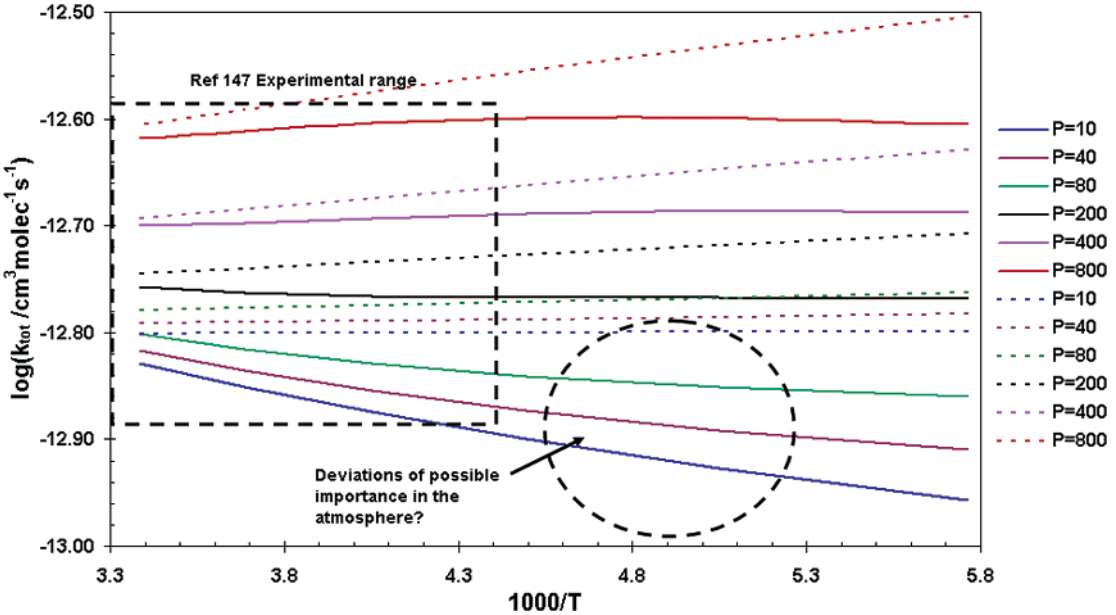

Figure 11. Comparison of analytical representations of the rate coefficient for the reaction of OH with CO in the temperature range 175 < *T*/K < 300 and the pressure range 5 < $P(N_2)$/Torr < 800 from refs 146 (dotted lines) and 144 (full lines).

All thermochemical and master equation calculations were performed using the MultiWell[13,145] collection of programs for solving the master equation. For the pressure and temperatures ranges considered, quasi-steady-state conditions were achieved within 200 collisions or less, and in most cases 10^5 trials were sufficient to obtain 0.1% accuracy in the rate coefficients. Figure 10 shows an example of the computed fit to pressure dependence over a wide pressure range at 298 K.

Fitting the results to the NASA format yields the parameters in Table 2. McCabe et al.,[146] on the basis of experiments in the range $50 < P/\text{Torr} < 750$ and $220 < T/\text{K} < 400$, presented an analytical function to describe the rate constant for the OH + CO reaction. Their expression is in excellent agreement with the NASA format of Senosiain et al.[144] in their experimental regime. Evaluation of individual data points reported by McCabe et al.,[146] using the NASA format in Table 2, shows an average deviation of 2%. Some possibly important atmospheric deviations between the expressions of McCabe et al.[146] and Senosiain et al.[144] are seen in Figure 11 at lower temperatures and pressures.

4. Conclusions

The treatment of pressure-dependent reactions can be quite complex because of the need to account for the effects of energy transfer, angular momentum, and details of the potential energy surface. A good many researchers in fields including atmospheric and combustion chemistry are deeply engaged in extending knowledge in these areas. Experiments in the laboratory and in the atmosphere have been crucial to improving understanding. Efforts are underway to improve master equation methods and to use them in informing development of practical approximations. Although current master equation approaches are useful for analyzing experimental data, efforts are underway in several laboratories to make them predictive. Since computer and software capabilities are continuing to improve at a rapid pace, such a goal may be achievable in the not-so-distant future. However, that will require implementing practical two-dimensional master equations (which explicitly include angular momentum as well as internal energy), advances in electronic structure calculations, and a deeper understanding of both intra- and intermolecular energy transfer. New, high-quality experimental measurements will be needed on energy distributions, branching ratios, and rate constants over challenging ranges of both temperature and pressure. We live in exciting times!

5. Acknowledgments

D.M.G. thanks the NASA Upper Atmosphere Research Program for support through Grant NAG-2-1397-1 to Stanford University. J.R.B. thanks the NSF Atmospheric Chemistry Division and the Petroleum Research Fund (administered by the American Chemical Society) for partial support of this work. Special thanks go to our colleagues Gregory P. Smith, Keith D. King, and Lawrence L. Lohr for countless stimulating discussions.

6. References

(1) Seinfeld, J. H.; Pandis, S. N. *Atmospheric Chemistry and Physics*; John Wiley & Sons: New York, 1998.
(2) Finlayson-Pitts, B. J.; Pitts, J. N., Jr. *Chemistry of the Upper and Lower Atmosphere*; Academic Press: San Diego, 2000.
(3) Atkinson, R. *J. Phys. Chem. Ref. Data* **1994**, Monograph No. 2.
(4) Atkinson, R. *Atmos. Environ.* **2000**, *34*, 2063.
(5) Atkinson, R.; Baulch, D. L.; Cox, R. A.; Crowley, J. N.; Hampson, R. F.; Kerr, J. A.; Rossi, M. J.; Troe, J. Summary of Evaluated Kinetic and Photochemical Data for Atmospheric Chemistry; IUPAC, 2001.
(6) Sander, S. P.; Friedl, R. R.; DeMore, W. B.; Ravishankara, A. R.; Golden, D. M.; Kolb, C. E.; Kurylo, M. J.; Hampson, R. F.; Huie, R. E.; Molina, M. J.; Moortgat, G. K. Chemical Kinetics and Photochemical Data for Use in Stratospheric Modeling, Evaluation No. 13; Jet Propulsion Laboratory, 2000.
(7) Tardy, D. C.; Rabinovitch, B. S. *Chem. Rev.* **1977**, *77*, 369.
(8) Oref, I.; Tardy, D. C. *Chem. Rev.* **1990**, *90*, 1407.
(9) Robinson, P. J.; Holbrook, K. A. *Unimolecular Reactions*; Wiley-Interscience: New York, 1972.
(10) Forst, W. *Theory of Unimolecular Reactions*; Academic Press: New York, 1973.
(11) Gilbert, R. G.; Smith, S. C. *Theory of Unimolecular and Recombination Reactions*; Blackwell Scientific: Oxford, 1990.
(12) Holbrook, K. A.; Pilling, M. J.; Robertson, S. H. *Unimolecular Reactions*, 2nd ed.; Wiley: Chichester, 1996.
(13) Barker, J. R. *Int. J. Chem. Kinet.* **2001**, *33*, 232.
(14) Barker, J. R.; Yoder, L. M.; King, K. D. *J. Phys. Chem. A* **2001**, *105*, 796.
(15) Troe, J. *J. Chem. Phys.* **1977**, *66*, 4758.
(16) Troe, J. *J. Chem. Phys.* **1977**, *66*, 4745.
(17) Troe, J. *J. Chem. Phys.* **1992**, *97*, 288.
(18) Troe, J. *Chem. Rev.* **2003**, *103*, 4565 (in this issue).
(19) Oref, I. *J. Phys. Chem.* **1989**, *93*, 3.
(20) Hessler, J. P.; Ogren, P. J. *J. Phys. Chem.* **1996**, *100*, 984.
(21) Hessler, J. P. *J. Phys. Chem.* **1996**, *100*, 2141.
(22) Prezhdo, O. *J. Phys. Chem.* **1995**, *99*, 8633.
(23) Pilling, M. J. *Int. J. Chem. Kinet.* **1989**, *21*, 267.
(24) Pawlowska, I. Z.; Gardiner, W. C.; Oref, I. *J. Phys. Chem.* **1993**, *97*, 5024.
(25) Kazakov, A.; Wang, H.; Frenklach, M. *J. Phys. Chem.* **1994**, *98*, 10598.
(26) Wang, H.; Frenklach, M. *Chem. Phys. Lett.* **1993**, *205*, 271.
(27) Barker, J. R.; Ortiz, N. F. *Int. J. Chem. Kinet.* **2001**, *33*, 246.
(28) Barker, J. R. MultiWell Program Suite, version 1.3.2; Ann Arbor, MI, 2003 (http://aoss.engin.umich.edu/multiwell/).
(29) Gilbert, R. G.; Jordan, M. J. T.; Smith, S. C. UNIMOL Program Suite, Sydney, Australia, 1990.
(30) Vereecken, L.; Huyberechts, G.; Peeters, J. *J. Chem. Phys.* **1997**, *106*, 6564.
(31) Klippenstein, S. J.; Wagner, A. F.; Robertson, S. H.; Dunbar, R.; Wardlaw, D. M. VariFlex Software, version 1.0, 1999.
(32) Mokrushin, V.; Tsang, W. *ChemRate. A Calculational Data Base for Unimolecular Reactions*; National Institute of Standards and Technology: Gaithersburg, MD, 2000.
(33) Smith, S. C.; Diau, E. W.-G.; Schranz, H. W. UNIRATE, Energy and Angular Momentum Resolved Generalized Transition State Theory Fortran Code, 2001.
(34) Beyer, T.; Swinehart, D. F. *Comm. Assoc. Comput. Machines* **1973**, *16*, 379.
(35) Stein, S. E.; Rabinovitch, B. S. *J. Chem. Phys.* **1973**, *58*, 2438.
(36) Truhlar, D. G.; Garrett, B. C. *Acc. Chem. Res.* **1980**, *13*, 440.
(37) Benson, S. W. *Thermochemical Kinetics*, 2nd ed.; Wiley: New York, 1976.
(38) Smith, G. P.; Golden, D. M. *Int. J. Chem. Kinet.* **1978**, *10*, 489.
(39) Gorin, E. *Acta Physicochim., URSS* **1938**, *9*, 691.
(40) Donahue, N. M.; Mohrschladt, R.; Dransfield, T. J.; Anderson, J. G.; Dubey, M. K. *J. Phys. Chem. A* **2001**, *105*, 1515.
(41) Hippler, H.; Nasterlack, S.; Striebel, F. *Phys. Chem. Chem. Phys.* **2002**, *4*, 2959.
(42) Robertshaw, J. S.; Smith, I. W. M. *J. Phys. Chem.* **1982**, *86*, 785.
(43) Burkholder, J. R.; Hammer, P. D.; Howard, C. J. *J. Phys. Chem.* **1987**, *91*, 2136.
(44) Golden, D. M.; Smith, G. P. *J. Phys. Chem. A* **2000**, *104*, 3991.
(45) Cheng, B.-M.; Lee, J.-W.; Lee, Y.-P. *J. Phys. Chem.* **1991**, *95*, 2814.
(46) Nizkorodov, S. A.; Wennberg, P. O. *J. Phys. Chem. A* **2002**, *106*, 855.
(47) Golden, D. M.; Barker, J. R.; Lohr, L. L. *J. Phys. Chem. A* **2003**, submitted.
(48) Troe, J. *Int. J. Chem. Kinet.* **2001**, *33*, 878.

(49) Matheu, D. M.; Green, W. H., Jr. *Int. J. Chem. Kinet.* **2000**, *32*, 245.
(50) Anastasi, C.; Smith, I. W. M. *J. Chem.. Soc. Faraday Trans. 2* **1976**, *72*, 1459.
(51) Brown, S. S.; Talukdar, R. K.; Ravishankara, A. R. *Chem. Phys. Lett.* **1999**, *299*, 277.
(52) Dransfield, T. J.; Perkins, K. K.; Donahue, N. M.; Anderson, J. G.; Sprengnether, M. M.; Demerjian, K. L. *Geophys. Res. Lett.* **1999**, *26*, 687.
(53) Wine, P. H.; Kreutter, N. M.; Ravishankara, A. R. *J. Phys. Chem.* **1979**, *83*, 3191.
(54) Fulle, D.; Hamann, H. F.; Hippler, H.; Troe, J. *J. Chem. Phys.* **1998**, *108*, 5391.
(55) Donahue, N. M.; Dubey, M. K.; Mohrschladt, R.; Demerjian, K. L.; Anderson, J. G. *J. Geophys. Res.* **1997**, *102*, 6159.
(56) D'Ottone, L.; Campuzano-Jost, P.; Bauer, D.; Hynes, A. J. *J. Phys. Chem. A* **2001**, *105*, 10538.
(57) 1976 Standard Atmosphere Calculator; Digital Dutch, 2003.
(58) *U.S. Standard Atmosphere, 1976*; U.S. Government Printing Office: Washington, DC, 1976.
(59) Molina, M. J.; Rowland, F. S. *Nature* **1974**, *249*, 810.
(60) Wallington, T. J.; Schneider, W. F.; Sehested, J.; Nielsen, O. J. *J. Chem. Soc., Faraday Discuss.* **1996**, *100*, 55.
(61) Pinnock, S.; Shine, K. P.; Smyth, T. J.; Hurley, M. D.; Wallington, T. J. *J. Geophys. Res.* **1995**, *100*, 23227.
(62) Ingle, L. M. *Proc. West Virginia Acad. Sci.* **1968**, *40*, 1.
(63) Tromp, T. K.; Ko, M. K. W.; Rodriguez, J. M.; Sze, N. D. *Nature* **1995**, *376*, 327.
(64) Dixon, D. A.; Fernandez, R. STEP−HALOCSIDE/AFEAS Workshop, University College Dublin, Ireland, 1993.
(65) Schneider, W. F.; Wallington, T. J.; Barker, J. R.; Stahlberg, E. A. *Ber. Bunsen-Ges. Phys. Chem.* **1998**, *102*, 1850.
(66) Schneider, W. F.; Wallington, T. J. *J. Phys. Chem.* **1993**, *97*, 12783.
(67) Schneider, W. F.; Nance, B. I.; Wallington, T. J. *J. Am. Chem. Soc.* **1995**, *117*, 478.
(68) Wallington, T. J.; Hurley, M. D.; Schneider, W. F.; Sehested, J.; Nielsen, O. J. *Chem. Phys. Lett.* **1994**, *218*, 34.
(69) Somnitz, H.; Zellner, R. *Phys. Chem. Chem. Phys.* **2001**, *3*, 2352.
(70) Wallington, T. J.; Hurley, M. D.; Ball, J. C.; Kaiser, E. W. *Environ. Sci. Technol.* **1992**, *26*.
(71) Edney, E. O.; Driscoll, D. J. *Int. J. Chem. Kinet.* **1992**, *24*, 1067.
(72) Tuazon, E. C.; Atkinson, R. *J. Atmos. Chem.* **1993**, *16*, 301.
(73) Bednarek, G.; Arguello, G. A.; Zellner, R. *Ber. Bunsen-Ges. Phys. Chem.* **1996**, *100*, 445.
(74) Rattigan, O. V.; Rowley, D. M.; Wild, O.; Jones, R. L.; Cox, R. A. *J. Chem. Soc., Faraday Trans.* **1994**, *90*, 1819.
(75) Wallington, T. J.; Hurley, M. D.; Fracheboud, J. M.; Orlando, J. J.; Tyndall, G. S.; Sehested, J.; Møgelberg, T. E.; Nielsen, O. J. *J. Phys. Chem.* **1996**, *100*, 18116.
(76) Dibble, T. S. *J. Phys. Chem. A* **2002**, *106*, 6643.
(77) Barker, J. R. MultiWell Program Suite, version 1.2.3; Ann Arbor, MI, 2002 (http://aoss.engin.umich.edu/multiwell/).
(78) Wittig, C.; Nadler, I.; Reisler, H.; Noble, M.; Catanzarite, J.; Radhakrishnan, G. *J. Chem. Phys.* **1985**, *83*, 5581.
(79) Reisler, H.; Wittig, C. In *State-Resolved Simple Bond-Fission Reactions: Experiment and Theory*; Barker, J. R., Ed.; JAI Press: Greenwich, CT, 1992; Vol. 1, p 139.
(80) Orlando, J. J.; Tyndall, G. S.; Bilde, M.; Ferronato, C.; Wallington, T. J.; Vereecken, L.; Peeters, J. *J. Phys. Chem. A* **1998**, *102*, 8116.
(81) Vereecken, L.; Peeters, J. *J. Phys. Chem. A* **1999**, *103*, 1768.
(82) Vereecken, L.; Peeters, J.; Orlando, J. J.; Tyndall, G. S.; Ferronato, C. *J. Phys. Chem. A* **1999**, *103*, 4693.
(83) Orlando, J. J.; Tyndall, G. S.; Vereecken, L.; Peeters, J. *J. Phys. Chem. A* **2000**, *104*, 11578.
(84) Somnitz, H.; Zellner, R. *Phys. Chem. Chem. Phys.* **2000**, *2*, 1899.
(85) Somnitz, H.; Zellner, R. *Phys. Chem. Chem. Phys.* **2000**, *2*, 4319.
(86) Somnitz, H.; Zellner, R. *Phys. Chem. Chem. Phys.* **2000**, *2*, 1907.
(87) Darnall, K. R.; Carter, W. P. L.; Winer, A. M.; Lloyd, A. C.; Pitts, J. N., Jr. *J. Phys. Chem.* **1976**, *80*, 1948.
(88) Lightfoot, P. D.; Cox, R. A.; Crowley, J. N.; Destriau, M.; Hayman, G. D.; Jenkin, M. E.; Moortgat, G. K.; Zabel, F. *Atmos. Environ.* **1992**, *26A*, 1805.
(89) Roberts, J. M. *Atmos. Environ.* **1990**, *24A*, 243.
(90) Wallington, T. J.; Nielsen, O. J.; Sehested, J. Reactions of organic peroxy radicals in the gas phase. In *Peroxyl Radicals*; Alfassi, Z. B., Ed.; John Wiley & Sons: Chichester, UK, 1997; p 113.
(91) Chow, J. M.; Miller, A. M.; Elrod, M. J. *J. Phys. Chem. A* **2003**, *107*, 3040.
(92) Atkinson, R.; Aschmann, S. M.; Carter, P. L.; Pitts, J. N., Jr. *J. Phys. Chem.* **1982**, *86*, 4563.
(93) McGrath, M. P.; Rowland, F. S. *J. Phys. Chem.* **1994**, *98*, 1061.
(94) McGrath, M. P.; Rowland, F. S. *J. Phys. Chem.* **1996**, *100*, 4815.
(95) Sumathy, R.; Peyerimhoff, S. D. *J. Chem. Phys.* **1997**, *107*, 1872.
(96) Dixon, D. A.; Feller, D.; Zhan, C.-G.; Francisco, J. S. *J. Phys. Chem. A* **2002**, *106*, 3191.
(97) Xia, W. S.; Lin, M. C. *J. Chem. Phys.* **2001**, *114*, 4522.
(98) Lohr, L. L.; Barker, J. R.; Shroll, R. M. *J. Phys. Chem. A* **2003**, *107*, 7429.
(99) Ellison, G. B.; Blanksby, S. J.; Jochnowitz, E. B.; Stanton, J. F. *J. Phys. Chem. A* **2003**, in preparation.
(100) Zhang, D.; Zhang, R.; Park, J.; North, S. W. *J. Am. Chem. Soc.* **2002**, *124*, 9600.
(101) O'Brien, J. M.; Czuba, E.; Hastie, D. R.; Francisco, J. S.; Shepson, P. B. *J. Phys. Chem. A* **1998**, *102*, 8903.
(102) Barker, J. R.; Lohr, L. L.; Shroll, R. M.; Reading, S. *J. Phys. Chem. A* **2003**, *107*, 7434.
(103) Greenhill, P. G.; Gilbert, R. G. *J. Phys. Chem.* **1986**, *90*, 3104.
(104) Forst, W. *J. Phys. Chem.* **1972**, *76*, 342.
(105) Atkinson, R.; Carter, W. P. L.; Winer, A. M. *J. Phys. Chem.* **1983**, *87*, 2012.
(106) Atkinson, R.; Aschmann, S. M.; Carter, W. P. L.; Winer, A. M.; Pitts, J. N., Jr. *Int. J. Chem. Kinet.* **1984**, *16*, 1085.
(107) Barker, J. R.; Toselli, B. M. *Int. Rev. Phys. Chem.* **1993**, *12*, 305.
(108) Golden, D. M. *Int. J. Chem. Kinet.* **2003**, *35*, 206.
(109) Bloss, W. J.; Nickolaisen, S. L.; Salawitch, R. J.; Friedl, R. R.; Sander, S. P. *J. Phys. Chem. A* **2001**, *105*, 11226.
(110) Trolier, M.; Mauldin, R. L., III; Ravishankara, A. R. *J. Phys. Chem.* **1990**, *94*, 4896.
(111) Zhu, R. S.; Lin, M. C. *J. Chem. Phys.* **2003**, *118*, 4094.
(112) Ung, A. Y. M.; Back, R. A. *Can. J. Chem. Rev. Can. Chim.* **1964**, *42*, 753.
(113) Dryer, F.; Glassman, I.; Naegeli, D. *Comb. Flame* **1971**, *17*, 270.
(114) Smith, I. W. M.; Zellner, R. *J. Chem. Soc., Faraday Trans. 2* **1973**, *69*, 1617.
(115) Smith, I. W. M. *Chem. Phys. Lett.* **1977**, *49*, 112.
(116) Jacox, M. E. *J. Chem. Phys.* **1988**, *88*, 4598.
(117) Ruscic, B.; Litorja, M. *Chem. Phys. Lett.* **2000**, *316*, 45.
(118) Ruscic, B.; Schwarz, M.; Berkowitz, J. *J. Chem. Phys.* **1989**, *91*, 6780.
(119) Scherer, N. F.; Sipes, C.; Bernstein, R. B.; Zewail, A. H. *J. Chem. Phys.* **1990**, *92*, 5239.
(120) Radford, H. E.; Wei, W.; Sears, T. J. *J. Chem. Phys.* **1992**, *97*, 3989.
(121) Sears, T. J.; Fawzy, W. M.; Johnson, P. M. *J. Chem. Phys.* **1992**, *97*, 3996.
(122) Sears, T. J.; Radford, H. E.; Moore, M. A. *J. Chem. Phys.* **1993**, *98*, 6624.
(123) Petty, J. T.; Harrison, J. A.; Moore, C. B. *J. Phys. Chem.* **1993**, *97*, 11194.
(124) Petty, J. T.; Moore, C. B. *J. Chem. Phys.* **1993**, *99*, 47.
(125) Ruscic, B.; Wagner, A. F.; Harding, L. B.; Asher, R. L.; Feller, D.; Dixon, D. A.; Peterson, K. A.; Song, Y.; Qian, X. M.; Ng, C. Y.; Liu, J. B.; Chen, W. W. *J. Phys. Chem. A* **2002**, *106*, 2727.
(126) Duncan, T. V.; Miller, C. E. *J. Chem. Phys.* **2000**, *113*, 5138.
(127) Yu, H. G.; Muckerman, J. T.; Sears, T. J. *Chem. Phys. Lett.* **2001**, *349*, 547.
(128) Zhu, R. S.; Diau, E. G. W.; Lin, M. C.; Mebel, A. M. *J. Phys. Chem. A* **2001**, *105*, 11249.
(129) Wooldridge, M. S.; Hanson, R. K.; Bowman, C. T. *Int. J. Chem. Kinet.* **1994**, *26*, 389.
(130) Vandooren, J.; VanTiggelen, P. J.; Pauwels, J. F. *Comb. Flame* **1997**, *109*, 647.
(131) Fulle, D.; Hamann, H. F.; Hippler, H.; Troe, J. *J. Chem. Phys.* **1996**, *105*, 983.
(132) Frost, M. J.; Sharkey, P.; Smith, I. W. M. *J. Phys. Chem.* **1993**, *97*, 12254.
(133) Frost, M. J.; Sharkey, P.; Smith, I. W. M. *Faraday Discuss.* **1991**, 305.
(134) DeMore, W. B.; Sander, S. P.; Golden, D. M.; Hampson, R. F.; Kinylo, M. J.; Howard, C. J.; Ravishankara, A. R.; Kolb, C. E.; Molina, M. J. Chemical Kinetics and Photochemical Data for use in Stratospheric Modeling; NASA-JPL, 1997.
(135) Atkinson, R.; Baulch, D. L.; Cox, R. A.; Hampson, R. F.; Kerr, J. A.; Troe, J. *J. Phys. Chem. Ref. Data* **1989**, *18*, 881.
(136) Baulch, D. L.; Cobos, C. J.; Cox, R. A.; Esser, C.; Frank, P.; Just, T.; Kerr, J. A.; Pilling, M. J.; Troe, J.; Walker, R. W.; Warnatz, J. *J. Phys. Chem. Ref. Data* **1992**, *21*, 411.
(137) Brunning, J.; Derbyshire, D. W.; Smith, I. W. M.; Williams, M. D. *J. Chem. Soc., Faraday Trans. 2* **1988**, *84*, 105.
(138) Larson, C. W.; Stewart, P. H.; Golden, D. M. *Int. J. Chem. Kinet.* **1988**, *20*, 27.
(139) Mozurkewich, M.; Benson, S. W. *J. Phys. Chem.* **1984**, *88*, 6435.
(140) Troe, J. Modeling the Temperature and Pressure Dependence of the Reaction HO+CO=HOCO=H+CO2. Presented at the 27th Symposium (International) on Combustion, 1998.
(141) Kudla, K.; Schatz, G. C.; Wagner, A. F. *J. Chem. Phys.* **1991**, *95*, 1635.
(142) Golden, D. M.; Smith, G. P.; McEwen, A. B.; Yu, C. L.; Eiteneer, B.; Frenklach, M.; Vaghjiani, G. L.; Ravishankara, A. R.; Tully, F. P. *J. Phys. Chem. A* **1998**, *102*, 8598.
(143) Kudla, K.; Schatz, G. C. *J. Phys. Chem.* **1991**, *95*, 8267.
(144) Senosiain, J. P.; Musgrave, C. B.; Golden, D. M. *Int. J. Chem. Kinet.* **2003**, *35*, 464.
(145) Barker, J. R. MultiWell-1.1.3, version 1.1.3; Ann Arbor, MI, 2001 (http://aoss.engin.umich.edu/multiwell/).

(146) McCabe, D. C.; Gierczak, T.; Talukdar, R. K.; Ravishankara, A. R. *Geophys. Res. Lett.* **2001**, *28*, 3135.
(147) Perry, R. A.; Atkinson, R.; Pitts, J. N. *J. Chem. Phys.* **1977**, *67*, 5577.
(148) DeMore, W. B. *Int. J. Chem. Kinet.* **1984**, *16*, 1187.
(149) Atkinson, R.; Baulch, D. L.; Cox, R. A.; Hampson, R. F. J.; Kerr, J. A.; Rossi, M. J.; Troe, J. *J. Phys. Chem. Ref. Data* **1997**, *26*, 1329.

CR020655D